RSC Advances

ROYAL SOCIETY OF CHEMISTRY

www.rsc.org/advances

Gel Polymer Electrolyte Based on the Novel Synthesized Matrix of Self-doped Polymer of h-poly(methyl methacrylate-vinyl trismethoxy silane)

Yun Huang[*a,] Rui Huang[a], Shengdong Gong[a], Haijun Cao[*b], Yuanhua Lin[a], Man Yang[a], Xing Li[a]

[a] School of Materials Science and Engineering, Southwest Petroleum University, Chengdu, 610500. China.

[b] Institute of Blood Transfusion, Chinese Academy of Medical Sciences, Chengdu, 610052, China.

---

[*] Corresponding author. Tel.: +86 28 83037409.
E-mail address: huangyun982@163.com (Y. Huang).
chj007@163.com (H. Cao).

Abstract: In order to incorporate inorganic nano-particle into gel polymer electrolyte (GPE) in the form of chemical bond to improve electrolyte performances, the monomers of methyl methacrylate (MMA) and vinyl trismethoxy silane (VTMS) were chosen to synthesize the novel self-doped polymer of h-poly(methyl methacrylate-vinyl trismethoxy silane) (h-P(MMA-VTMS)), and then the obtained polymer was used as matrix to prepare GPE. By the characterization of the resulted polymer, the composition and structure are conformed to the design concept, and the self-doped polymer is amorphous and possesses two different glass transition temperatures (T_g) and the better thermal stability. From the investigation of the prepared GPE, it is thermal stable in the temperature range from 30°C to 100°C; the ionic conductivity reaches the level of 10^{-4}S/cm at room temperature; For the 50wt.%GPE system, the variation of ionic conductivity displays an Arrhenius behavior in the temperature range from 30°C to 60°C; the higher lithium ion transference number is 0.42; the compatibility with lithium metal anode is better; the electrochemical stability is stable up to 5.2 V versus Li /Li^+.

Keywords: gel polymer electrolyte; methyl methacrylate; vinyl trismethoxy silane; self-doped polymer

Introduction

Lithium ion battery has gained an extensive application in the last decade as the energy storage device of portable digital products such as cell phone, computer, camera, etc [1-4]. At present, the lithium ion battery products selling in market mostly and mainly are prepared using liquid electrolyte which can provide high ionic conductivity, favorable compatibility with electrode and lower cost [5-7]. But on the other hand, owing to several shortcomings such as leakage, flammability and chemical instability, vigorous research efforts have been devoted to replace liquid electrolyte with solid fast ion conductors [6-7]. Among various solid fast ion conductor candidates such as solid polymer electrolyte (SPE) [7-8], ceramic electrolyte (CE) [9-11] and gel polymer electrolyte (GPE) [12-13], GPE is superior to other electrolytes and has garnered increasing attention as it provides not only satisfying ionic conduct and favorable interfacial compatibility with electrode but also reliable safety, high modularity and shape design space within the cell geometry [14-17].

From the first GPE research in 1994, the improvement of GPE performances such as ionic conductivity at room temperature, mechanical property, thermal stability, electrochemical stability and C-rate performance of cells has been carried out for twenty years. The most efficient method to obtain prospective result is the composition and structure design of polymer matrix. It is obvious that each single polymer such as PMMA [18-20], PAN [21-22], PEO [23-24], PVDF [25-26], etc, is favorite to provide GPE some curtain property and do not meet all requirements of GPE. So in some reports, these monomers such as MMA, AN, EO and VDF were chosen to synthesize copolymer used as matrix for GPE. In addition, designing special structure such as comb-shape [27], graft-shape [28-29], star-shape [30] and crosslink-shape [31] for polymer matrix is also a very interesting measure. Each structure can promise characteristic property in one aspect. So in some recent researches, to achieve the wonderful effect, combining both method together to design polymer matrix with certain composition and signature structure is becoming popular. But this kind of method is undoubtedly expensive, which certainly limits the widespread appliance of battery. Besides, many polymer matrix designed do not mostly be achieved without appropriate synthesis route.

To quest for improving comprehensive properties of GPE by incorporating inorganic nanoparticles into electrolyte system is another promising method. The inorganic nanoparticles includes metal oxide, such as MgO [32-33], ZnO [34], Al_2O_3 [32-35], TiO_2 [34-38,42], ZrO_2 [39-40], SnO_2[41] and CeO_2 [42], inorganic oxide SiO_2 [15,43-48], carbon nanotube [14], clay mineral [29] found in many references. However, the high surface energy from large surface area of all inorganic nanoparticles usually leads to particle agglomeration, which negates any benefits associated with the nanoparticles [49]. In order to overcome the aforementioned distinct drawback, a facile and efficient route to decrease the surface energy of inorganic nanoparticles is to change the hydrophilic to hydrophobic nature of nanoparticles by organic modification on the surface of particles using various monomers or polymer with some curtain chemical structure and functionality. Even so, incorporating inorganic nanoparticles into electrolyte system remains deeply ambivalent. There are two basic reasons: one is that the method of organic modification on nanoparticles surface just can solve the agglomeration problem to some extent, and the other is the organic modification drives up cost which finally limits the larger-scale application of GPE.

Bearing the two facts mentioned above, we predict one polymer which can be synthesized easily with simple route and is one kind of potential excellent matrix for GPE. The predicted polymer is based on the monomer of methyl methacrylate (MMA) and vinyl-trismethoxy silane (VTMS). MMA belongs to acrylate monomer and polyacrylate is one kind of the most extensive and outstanding polymer used as matrix for GPE. VTMS provides the very special functional group of methoxy silane which can change to segment of -Si-O-Si-. The formed segment can behave as inorganic nanopaticles and produces the similar modification function in GPE. In addition, the obtained -Si-O-Si- is chemically linked into the chain of the designed polymer and reaches the extent of molecule dispersion level, which completely resolves the agglomeration drawback of inorganic particles filler added physically. In the case of performance improvement, the train of thought of designing polymer matrix used for GPE will definitely attract a great deal of attention.

According to the above concept, in our present work, MMA and VTMS were chosen to synthesize copolymer of P(methylmethacrylate-co-vinyl-trismethoxy silane) (P(MMA-VTMS)), and then the obtained copolymer was hydrolyzed in acid solution to generate silanol group. At last in higher temperature, the dehydration condensation polymerization between silanol was carried out, and the segment of -Si-O-Si- was appeared in the resulted polymer. Because of the function of -Si-O-Si-, the ultimate product designated as h-P(MMA-VTMS) was obviously the so-called self-doped polymer. We demonstrate here for the first time the self-doped polymer of h-P(MMA-VTMS) as one new viable matrix to prepare GPE. So there were two projects in the manuscript. Firstly, the self-doped polymer of h-P(MMA-VTMS) was needed to be evidenced by Fourier Transform Infrared spectroscopy (FTIR), Nuclear Magnetic Resonance (NMR), X-ray diffraction (XRD), differential scanning calorimetry (DSC) and thermogravimetric analysis (TGA). Secondly, the manuscript discussed the results related to the most important properties of GPE. In this research, we reported a preliminary study demonstrating the feasibility of GPE based on the matrix of self-doped polymer of h-P(MMA-VTMS).

Experimental

Materials

Methyl methacrylate (MMA) (AR), methanol (AR), acetone (AR), hydrochloric acid (AR), toluene (AR), 2,2'-Azobis(2-methylpropionitrile) (AIBN,AR), lithium perchlorate (anhydrous, AR), propylene carbonate(PC) (AR) were obtained from Chengdu Kelong Company. Vinyl-trismethoxy silane(VTMS,CP) was obtained from Najing UP Chemical.

Synthesis of the self-doped polymer of h-P(MMA-VTMS)

P(MMA-VTMS) was synthesized using solution polymerization in a 3 neck glass reactor equipped with a nitrogen inlet, a reflux condenser, an additional funnel and a mechanical stirrer. AIBN in the amount of 2wt.% was used as a free-radical initiator. 50 ml MMA and 9.7 ml VTMS were mixed in 150 ml toluene under stirring at 80°C. The polymerization was continued for 10h with vigorous agitation. The resulted product was poured into hydrochloric acid in the amount of 1.5 vl.% for the hydrolysis. After stirring vigorously for 3h, the emulsion product was firstly precipitated with methanol and then was washed with deionized water, and at last was transferred into the vacuum drying oven to remove impurities such as residual monomers and emulsifier. The self-doped polymer h-P(MMA-VTMS) in the form of white powder was finally obtained by dehydration condensation polymerization in a vacuum oven at 80°C for 1h. Scheme.1 reveals the ideal synthesis route of the self-doped polymer h-P(MMA-VTMS). The structure of h-P(MMA-VTMS) also is shown in Scheme.2.

Preparation of GPE film

The preparation procedure of GPE film included two steps. Step one, a liquid electrolyte was prepared. Liquid electrolyte was obtained by dissolving $LiClO_4$ into the plasticizer of PC, and the lithium salt concentration was 1 $molL^{-1}$. Step two, GPE film was produced. Desired amount of the self-doped polymer h-P(MMA-VTMS) was added into acetone to form suspension solution. The suspension was kept in sealed cup under magnetic agitation until the viscosity of acetone was increased up to a stable and changeless extend, and polymer powder also reached the complete gelation state after one day. The liquid electrolyte was then added into the solution. After stirred for 1h, the mixture was casted onto a PTFE plate to allow acetone to evaporate slowly at room temperature. Five days later, the resulted film was in transparent, homogenous and mechanically stable. The weight percent of polymer matrix in GPE was varied as 50wt.%, 55wt.%, 60wt.% and 65wt.%. The average thickness of GPE film is 800μm.

Characterization

The structure of the self-doped polymer was characterized by FTIR (Perkin Elmer Spectrograph) in the range of 4000~400cm^{-1}. NMR spectra were recorded in acetone-d$_6$ on a Bruker AV Ⅱ-400 Spectrometer, and tetramethylsilane (TMS) was used as the internal reference for chemical shifts. XRD patterns were obtained by Rigaku miniflex diffractometer (Cu Kα, λ= 1.5418) at room temperature. DSC was conducted on METTLER TOLEDO with the heating rate of 10℃min^{-1}. TGA was conducted on METTLER TOLEDO with the heating rate of 10℃/min under air atmosphere. The ionic conductivity of GPE was characterized by electrochemical impedance spectra (EIS) measurement (CHI-660D electrochemical work station, China) in an ordinary cell composed of a Teflon tube and two identical stainless steel electrodes (diameter=1cm). The frequency range of the signal was from 0.1 Hz to 100 KHz, and the amplitude of the alternative signal was 10 mV. The cell was placed in sealed plastic bag immersed in water bath pool to control temperature. The reductive stability was determined on CHI-660D by EIS using the symmetrical cell Li/GPE/Li with amplitude of 5 mV and frequencies from 0.1 kHz to 100 Hz. The oxidative stability of GPE was determined on CHI-660D by linear sweep voltammetry (LSV) using the cell Li/GPE/SS, in which the SS was used as working electrode, the lithium as the reference and the counter electrodes. The scanning rate is 5mV s^{-1}. All assembly processes were carried out in a glove box that was filled with argon.

Results and discussion

Structure and properties of the self-doped polymer

FTIR spectrum structural analysis

Fig.1 presents the FTIR spectrum of self-doped polymer h-P(MMA-VTMS). It can be seen that the polymer loses the characteristic peaks at 1660~1640 cm^{-1} and 895~885 cm^{-1} for C=C group. This indicates that the resulted polymer is firstly formed through breaking of C=C bonds in each monomer, as shown in the first step in Scheme.1. The characteristic peak at 1731 cm^{-1} is the C=O group in polymer. And the symmetric stretching vibration of the siloxane (-Si-O-Si-) group appears at 1143 cm^{-1}. The peaks at 1058 cm^{-1} and 959 cm^{-1} are for -Si-O-C- group, and reflect that some methoxy groups in VTMS are not hydrolyzed. The weak peak at 866 cm^{-1} is the designation of -Si-OH group and verifies that not all -Si-OH group carry out dehydration condensation reaction in the final step in Scheme.1. In addition, the peak area ratio of -Si-O-Si-, -Si-O-C- and -Si-OH can supply the definite percentage value of each specific group in the self-doped polymer of h-P(MMA-VTMS). So by quantitative analysis, the percentage value of -Si-O-Si-, -Si-O-C- and -Si-OH are 63.7%, 25.2% and 11.1% in h-P(MMA-VTMS) , respectively. So Scheme.1 and Scheme.2 just reflect the ideal reaction results. With the same method, the monomer ration of MMA and VTMS is 7:3 which is determined by the peak area ratio of C=O group in MMA and Si group (-Si-O-Si-, -Si-O-C- and -Si-OH) in VTMS, so in Scheme.1 the value of m:n is7:3.

NMR of self-doped polymer

Fig.2 presents the ^{1}H-NMR spectrum of the self-doped polymer of h-P(MMA-VTMS) synthesized as the matrix of GPE. The peaks appears between 7.15-7.30 ppm higher chemical shifts come from the aromatic protons (H_f) which is the residual toluene used as solvent in polymerization. The peak at intermediate chemical shift of 3.64 ppm is identified as the proton (H_a) neighbored ester group. There are many peaks shown in the low chemical shifts between 0.50-2.50 ppm are designated to represent the protons from methyl (H_b in the range of 0.88 to 1.06 ppm and H_e at 2.33 ppm), methylene (H_d in the range of 1.89-1.98 ppm) and methane (H_c in the range of 2.05-2.08 ppm), respectively. In addition, the solvent of Acetone-d6 used here contains trace amount of water expresses a sharp peak at 2.85 ppm [50].

The ^{29}Si-NMR spectrum of the self-doped polymer, as shown in **Fig.3**, shows a very wide peak in the range from -60 ppm to -140 ppm. The wide peak is the overlap result of many sharp peaks: the inorganic SiO_2-like structure of Q^n=Si-$(OSi)_n$-OH_{4-n} (n=2-4) produced in the self-doped polymer has peaks at around -110 ppm for Q^4, around -100 ppm for Q^3 and around -90 ppm for Q^2; the organic siloxane structure of T^n=R-Si-$(OSi)_n$-OH_{3-n} (n=1-3) has peaks at around -70 ppm for T^3 and around -60 ppm for T^2. All these peaks indicate that we obtain the designed polymer matrix.

FTIR and NMR spectra reveal that the self-doped polymer h-P(MMA-VTMS) is successfully synthesized.

Thermal property of self-doped polymer

Fig.4 shows the DSC thermogram obtained for the self-doped polymer h-P(MMA-VTMS). Two different glass transition temperatures (T_g) are obviously observed, which indicates that there are two phases in the polymer. One is organic phase from MMA portion, and the other is inorganic phase from -Si-O-Si- segment. The lower slight inflection temperature at 85.4°C is originated from the organic phase and the higher sharp temperature at 178°C is attributed to the inorganic phase. The evidence also proves the inorganic modification by incorporation of -Si-O-Si- segment in chemical bond in polymer h-P(MMA-VTMS).

The thermal stability of the self-doped polymer h-P(MMA-VTMS) is determined by TGA under air atmosphere from room temperature to 500°C. The result is shown in **Fig.5**. The thermal degradation curve displays a three stage decomposition trend starting at 120℃. The first stage starts from 120℃ to 220℃ with the weight loss due to the evaporation of residual solvent inside the polymer matrix; the second stage from 260℃ to 310℃ is due to the decomposition of organic phase in polymer; the third stage from 340℃to 420℃ with a quick and large degradation process is attributed to the inorganic phase decomposition in h-P(MMA-VTMS). Therefore, the obtained polymer has favorable thermal stability which totally meets the thermal requirement of lithium ion battery. These results further proves that the synthesized polymer definitely and successfully is doped self by chemical bond connect form.

XRD analysis

Fig.6 shows XRD pattern of self-doped polymer and is used to investigate the structure of the synthesized polymer. At the 2θ=29.4°、42.7°, only two weak peaks are observed, so the structure of polymer is amorphous state.

Properties of GPE system

Based on the above analysis, the synthesized self-doped polymer h-P(MMA-VTMS) are demonstrated. The following content will focus on the research of GPE with the matrix of h-P(MMA-VTMS).

Thermal stability of GPE system

TGA was used to measure the thermal stability of the GPE for application in the lithium ion batteries. **Fig.7** shows the TGA curves of these GPEs with four different polymer matrix weights.

Four GPEs almost do not show weight loss and the thermal stability reach up to the temperature of 120℃. The onset temperature for the degradation of four GPEs is close to 140℃, which indicates that no component is volatile in GPE till 140℃. The temperature range of stability is wide enough for GPE to be applied as electrolyte in lithium ion batteries.

In these curves, there is one very interesting and important phenomenon. That is on blending with plasticizer of PC and lithium salt of $LiClO_4$, the temperature point of thermal stability of four GPEs do not completely change compared with that of pure polymer matrix. The reason may be that the plasticizer molecule totally integrated into the chains of polymer, and one kind of strong attraction force is formed between plasticizer and polymer chain, which likely makes two components become one material.

DSC of GPE system

DSC curves of the self-doped polymer GPE systems are depicted in **Fig.8**, from which DSC curves do not appear any obvious endothermic peak. This phenomenon indicates that four kinds of self-doped polymer GPE system are stable in the temperature range from 30˚C to 100˚C, which satisfies the higher temperature requirement in actual cell product application.

XRD analysis

In order to characterize the structure transformation message of components in GPE and then investigate the interaction between them, XRD analysis is performed for lithium salt of $LiClO_4$ and 50wt.% GPE. The sharpness of XRD (**Fig.9** (a)) reflects clearly good crystallinity of lithium salt with a long range order. But in **Fig.9** (b), the peaks of lithium salt in XRD pattern of 50wt.% GPE disappears completely, which is the result of total disassociation of lithium salt. In addition, the pattern expresses two weak peaks at $2\theta=29.4°$, $42.7°$, which is similar to that of pure self-doped polymer presented in **Fig.6**. This suggests that the self-doped polymer matrix do not change in the aspect of structure and just acts as skeleton support in GPE system. The opinion is also verified by the above thermal analysis. And in addition, the lithium salt disassociation is the result of only interaction with plasticizer of PC.

Electrochemical property

GPE system is then investigated using the important factor of ionic conductivity (σ). The ionic conductivity measurement of GPE is carried out from the complex EIS curve and can be obtained from Equation (1).

$$\sigma = \frac{L}{R_b S} \qquad (1)$$

Where L (cm) is the thickness of GPE, R_b (Ω) is the electrolyte bulk resistance and S (cm^2) is the contact area between GPE and stainless steel (SS) square.

In equation (1), the parameter of R_b usually is retrieved from the EIS. The EIS of GPEs based on the synthesized self-doped polymer h-P(MMA-VTMS) are presented in **Fig.10**.

From **Fig.10**, the R_b value is gradually increased with the weight percent of polymer matrix in GPE, which is a typical trend for GPE. Usually the R_b value is inversely proportional to the amount of plasticizer in GPE. The reason is that the more amount plasticizer endows the charge carries of lithium ion with the easier movement ability. So the ionic conductivity of GPEs with the polymer amount percent of 65wt.%, 60wt.%, 55wt.% and 50wt.% are 2.88×10^{-5} Scm^{-1}, 6.89×10^{-5} Scm^{-1}, 1.48×10^{-4}Scm^{-1} and 3.76×10^{-4} Scm^{-1}, respectively. But in the EIS shapes, there is a significant difference. That is, the semicircle part in EIS of GPE gently appears with the polymer amount, which indicates that the interface impedance between electrolyte and stainless steel electrode ascends. It was not totally difficult to understand the trend. When polymer amount is increased, the plasticizer amount is conversely decreased in GPE, which definitely reduces the affinity between electrolyte and electrode, and ultimately the interface impedance raises gradually.

The relationship between temperature and ion conductivity is used to analyze the mechanism of ionic conduction in self-doped polymer GPE membranes in the temperature range from 30°C to 60°C, which is shown in **Fig.11** and **12**. Based on the result of better ionic conductivity and self-standing ability, the flowing research will be established on the kind of 50wt.%GPE system.

From the insert in **Fig.11**, the electrolyte bulk resistance R_b(Ω) is continuously increased with temperature. It is very easy to understand the relation. In GPE system, the motion of polymer chain is the movement driving force of current carriers of lithium ion, and the higher temperature endows the polymer chain with more flexibility and enhances segmental mobility [51], which undoubtedly and ultimately is beneficial to improve the ionic conductivity. The ionic conductivity is reasonably determined by the Arrhenius equation, which can be written as follows:

$$\sigma = A\exp(-E_a / \kappa T) \tag{2}$$

Where σ is the ionic conductivity; A is the pre-exponential factor; E_a is the activation energy; κ is the Boltzmann constant and T is the absolute temperature.

Fig.12 typically depicts the temperature dependence of the ionic conductivity of 50wt.% GPE system. The fitting line shows satisfying linear correlation parameter R^2 of 0.975 in Table1, so the variation of the ionic conductivity displays a basic Arrhenius behaviour over the temperature range from 30℃ to 60℃ upwards. The highest measured conductivity of the membrane at 60℃ was 1.32×10^{-3} $\mathrm{Scm^{-1}}$. In addition, the lithium movement active energy E_a in the GPE is 68.9kJ $\mathrm{mol^{-1}}$.

Table 1

The linear fitting data of lg σ vs.10^3T^{-1}

Linear fitting equation	E_a(kJ $\mathrm{mol^{-1}}$)	Linear correlation parameter R^2
lg σ = $-3.59\times10^3T^{-1}+8.07$	68.9	0.975

Lithium ion transference number ($t_{Li}{}^{+}$) is measured using a symmetric cell of Li/50wt.%GPE/Li by the DC polarization method combined with EIS method, as described by Bruce and Vincent [52]. It can be obtained according to the following equation:

$$t_{Li^+} = \frac{I_s(\Delta V - R_0 I_0)}{I_0(\Delta V - R_s I_s)} \tag{3}$$

Where I_0 and I_s are the initial and steady current, respectively; R_0 and R_s are the initial interfacial and steady-state resistance, respectively; $\triangle V$ is the DC voltage applied.

$t_{Li}{}^{+}$ is considered as an important parameter to appreciate the performance of polymer electrolytes. In this paper, the lithium ion transference number of GPE is 0.42, which is much higher than that of many commercial separator and GPEs reported in references.

The satisfying compatibility of GPE with lithium anode, which can be reflected by the interfacial impedance, is a key factor of application in lithium ion battery. In **Fig. 14** the variations of impedance spectra with the storage time for the cell using the self-doped polymer based 50wt.%GPE are presented. The symmetrical Li/50wt.%GPE /Li cell has one kind of equivalent circuit expressed as R_b+R_{ct}//$\mathrm{CPE_1}$+R_p//$\mathrm{CPE_2}$ (+ represents series connection;// represents parallel connection). R_b, R_{ct} and R_p are the bulk resistance of GPE, the charge transfer resistance between

Li anode and passive layer and the resistance of passive layer, respectively. The passive layer is formed by the interaction of lithium metal with the plasticizer of PC in the GPE. CPE_1 and CPE_2 are the interfacial double layer capacitor between Li and passive layer and the capacitor of passive layer, respectively. The interfacial resistance of R_i between lithium metal anode and GPE is the summation of R_{ct} and R_p. It can be seen that the interfacial resistance determined by the diameter of the semicircle exhibited in the impedance spectra increase with increasing storage time. With storage time, the thickness and structure of the formed passive layer is continuing to change, which leads to R_i increase.

The electrochemical potential window (i.e. working voltage range) is an important parameter of GPE evaluated from the point of view of application of electrochemical devices. And what is more important, the compatibility of GPE with cathode of lithium ion battery can be charactered by their electrochemical stability on stainless steel electrode under anodic oxidation. The working voltage range of the self-doped polymer GPE is determined by LSV using a Li/50wt.%GPE/SS cell. **Fig. 15** shows the current response of the working electrode. The anodic current onset of the oxidative decomposition of organic solvent such as EC (ethylene carbonate), PC (ethylene carbonate) and DMC (dimethyl carbonate) in liquid electrolyte is 4.4 V (vs.Li/Li^+) [53], whereas there is no obvious current through the working electrode up to 5.2V versus Li/Li^+, and then the current onset that is related to the decomposition of GPE is appeared when the electrode potential is higher than 5.2V (versus Li/Li^+). The improvement of electrochemical stability should be ascribed to the gelation of the liquid electrolyte. The gelation improves the stability of the electrolyte because of the interaction between liquid electrolyte and polymer, which restricts the free movement and the activity of the liquid electrolyte in GPE [52]. The result exhibits that the electrochemical stability window is 5.2V for the self-doped GPE. Definitely, in order to significantly improve the capacity and energy density of battery, the operation voltage of cathode materials must be firstly enhanced. However this approach usually is prevented because of the oxidation decomposition of electrolyte under higher working voltage over 4.5V. So the present adequate high electrochemical potential window make this kind of electrolyte potential choice for application in lithium ion batteries with a relatively board voltage cathode materials.

Conclusion

In this study, we successfully synthesized one novel self-doped polymer h-P(MMA-VTMS) by introduce -Si-O-Si- segment in chemical bond. The resulted self-doped polymer can be used as matrix to prepare GPE. GPE are thermal stable in the range temperature from 30°C to 60°C; the ionic conductivity reaches up to the level of 10^{-4} Scm^{-1} at room temperature; lithium ion transference number is 0.42; the electrochemical stability of GPE with electrode is satisfying. Considering these results, the investigated GPE appears as a promising candidate for lithium-ion batteries. The initial feasibility study presented here shows a promising strategy for designing self-doped polymer by incorporating inorganic modification in chemical bond. However, comprehensive work is still required to address the application in lithium ion batteries.

Acknowledgements

The authors gratefully acknowledge the financial support from the Key Fund Project of Sichuan Provincial Department of Education (15ZA0050), Open Fund for the Oil and Gas Materials Key Laboratory of Higher Education of Sichuan Province (x151514kc104) and the Innovative Research Team of Sichuan Provincial Department of Education (14TD0005).

References

[1] Y. Wang, J. Travas-Sejdic and R. Steiner, Solid State Ionics., 2002, 148, 443-449.

[2] M. Song, B.W. Cho, J. Cho and H. Rhee, J. Power Sources., 2002, 110, 209-215.

[3] H. Inaba, M. Iwaku, K. Nakase, H. Yasukawa, I. Seo and N. Oyama, Electrochim. Acta., 1995, 40, 227-232.

[4] S. Jeschke, M. Mutke, Z. Jiang, B. Alt and H.D. Wiemhofer, Chem. phys. chem., 2014, 15, 1761-1771.

[5] I. Nachev and M. Balkanski, Solid State Ionics., 1995, 78, 63-67.

[6] S. Sekhon, Solid State Ionics., 2003, 160, 301-307.

[7] K. Murata, S. Izuchi and Y. Yoshihisa, Electrochim. Acta., 2000, 45, 1501-1508.

[8] D. He, D.W. Kim, J.S. Park, S.Y. Cho and Y. Kang, J. Power Sources., 2013, 244, 170-176.

[9] K. Minami, A. Hayashi, S. Ujiie and M. Tatsumisago, Solid State Ionics., 2011, 192, 122-125.

[10] A.I.B. Rondão, S.G. Patrício, F.M.L. Figueiredo and F.M.B. Marques, Electrochim. Acta., 2013, 109, 701-709.

[11] C.C. Cook and M.J. Wagner, Electrochim. Acta., 2013, 89, 778-783.

[12] S.S. Sekhon, D.P. Kaur, J.S. Park and K. Yamada, Electrochim. Acta., 2012, 60, 366-374.

[13] S. Oh, D.W. Kim, C. Lee, M. Lee and Y. Kang, Electrochim. Acta., 2011, 57, 46-51.

[14] C. Tang, K. Hackenberg, Q. Fu, P.M. Ajayan and H. Ardebili, Nano Lett., 2012, 12, 1152-1156.

[15] Y. Fu, X. Ma, Q. Yang and X. Zong, Mater. Lett., 2003, 57, 1759-1764.

[16] A.S. Kamisan, T.I.T. Kudin, A.M.M. Ali and M.Z.A. Yahya, Electrochim. Acta., 2011, 57, 207-211.

[17] Q. Lu, J. Fang, J. Yang, G. Yan, S. Liu and J. Wang, J. Membr. Sci., 2013, 425-426, 105-112.

[18] J. Sharma and S. Sekhon, Solid State Ionics., 2007, 178, 439-445.

[19] Z. Osman, M.I. Mohd Ghazali, L. Othman and K.B. Md Isa, Results in Phys., 2012, 2, 1-4.

[20] J.P. Sharma and S.S. Sekhon, Mater. Sci. Eng. B., 2006, 129, 104-108.

[21] A. Gopalan, P. Santhosh, K. Manesh, J. Nho, S. Kim, C. Hwang and K. Lee, J Membr. Sci., 2008, 325, 683-690.

[22] M.M. Rao, J.S. Liu, W.S. Li, Y. Liang and D.Y. Zhou, J Membr. Sci., 2008, 322, 314-319.

[23] Y. Kang, K. Cheong, K. Noh, C. Lee and D. Seung, J. Power Sources., 2003, 119-121, 432-437.

[24] Z. Yue, I.J. McEwen and J.M.G. Cowie, Solid State Ionics., 2003, 156, 155-162.

[25] W. Li, Y. Xing, X. Xing, Y. Li, G. Yang and L. Xu, Electrochim. Acta., 2013, 112, 183-190.

[26] C.L. Cheng, C.C. Wan and Y.Y. Wang, J. Power Sources., 2004, 134, 202-210.

[27] P. Jannasch, Solid State Ionics., 2004, 166, 417-424.

[28] K. Inomata, K. Nakagawa, C. Fukuda, Y. Nakada, H. Sugimoto and E. Nakanishi, Polymer., 2010, 51, 793-798.

[29] K. Edelmann and B. Sandner, Polymer. 2005, 46, 397-406.

[30] H. Xie, D. Tao, X. Xiang, Y. Ou, X. Bai and L. Wang, J. Membr. Sci., 2015, 473, 226-236.

[31] M. Yang, W. Li, G. Wang and J. Zhang, Solid State Ionics., 2005, 176, 2829-2834.

[32] P.P. Prosini, P. Villano and M. Carewska, Electrochim. Acta., 2002, 48, 227-233.

[33] C. Wu, M. Lu, C. Tsai and H. Chuang, J. Power Sources., 2006, 159, 295-300.

[34] M. Yang, Y. Men, S. Li and G. Chen, Appl. Catal., A: General., 2012, 433-434, 26-34.

[35] A. Sarnowska, I. Polska, L. Niedzicki, M. Marcinek and A. Zalewska, Electrochim. Acta., 2011, 57, 180-186.

[36] J. Cao, L. Wang, Y. Shang, M. Fang, L. Deng, J. Gao, J. Li, H. Chen and X. He, Electrochim. Acta., 2013, 111, 674-679.

[37] J. Cao, L. Wang, M. Fang, Y. Shang, L. Deng, J. Yang, J. Li, H. Chen and X. He, Electrochim. Acta., 2013, 114, 527-532.

[38] J. Adebahr, A.S. Best, N. Byrne, P. Jacobsson, D.R. MacFarlane and M. Forsyth, Phys. Chem. Chem. Phys., 2003, 5, 720-725.

[39] D. Kéomany, J.-P. Petit and D. Deroo, Sol. Energy Mater. Sol. Cells., 1995, 36, 397-408.

[40] H. Nithya, S. Selvasekarapandian, P. Christopher Selvin, D. Arun Kumar, M. Hema and D. Prakash, Physcia. B., 2011, 406, 3367-3373.

[41] A. Subramania, N.T. Kalyana Sundaram, A.R. Sathiya Priya and G.V. Kumar, J. Membr. Sci., 2007, 294, 8-15.

[42] P. Zhang, H.P. Zhang, G.C. Li, Z.H. Li and Y.P. Wu, Electrochem. Commun., 2008, 10, 1052-1055.

[43] D. Kumar and S.A. Hashmi, J. Power Sources., 2010, 195, 5101-5108.

[44] J. Sharma and S. Sekhon, Solid State Ionics., 2007, 178, 439-445.

[45] Y. Lee, S.H. Ju, J. Kim, S.S. Hwang, J. Choi, Y. Sun, H. Kim, B. Scrosati and D. Kim, Electrochem. Commun., 2012, 17, 18-21.

[46] H. Jeong, E. Choi, S. Lee and J.H. Kim, J Membr. Sci., 2012, 415-416, 513-519.

[47] A. Chandra, A. Chandra and K. Thakur, Composites Part B: Eng., 2014, 60, 292-296.

[48] Y.H. Liao, M.M. Rao, W.S. Li, L.T. Yang, B.K. Zhu, R. Xu and C.H. Fu, J. Membr. Sci., 2010, 352, 95-99.

[49] M.E. Mackay, A. Tuteja, P.M. Duxbury, C. J. Hawker, B. Van Horn, Z. Guan, G. Chen and R.S. Krishnan, Sci., 2006, 311, 1740-1743.

[50] H.E. Gottlieb, V. Kotlyar and A. Nudelman, J. Org. Chem., 1997, 62, 7512-7515.

[51] M. Deka and A. Kumar, Electrochim. Acta., 2010, 55, 1836-1842.

[52] F. Cai, X. Zuo, X. Liu, L. Wang, W. Zhai and H. Yang, Electrochim. Acta., 2013, 106, 209-214.

[53] H. Xie, Y. Liao, P. Sun, T. Chen, M. Rao and W. Li, Electrochim. Acta., 2014, 127, 327-333.

Scheme.1. The ideal synthesis route of the self-doped polymer h-P(MMA-VTMS) (m:n=7:3).

Scheme.2. The ideal structure of the self-doped polymer h-P(MMA-VTMS).

Fig.1. FTIR spectrum of the self-doped polymer h-P(MMA-VTMS).

Fig.2. ^{1}H-NMR spectrum of the self-doped polymer of h-P(MMA-VTMS).

Fig.3. ^{29}Si-NMR spectrum of the self-doped polymer h-P(MMA-VTMS).

Fig.4. DSC curve of the self-doped polymer of h-P(MMA-VTMS).

Fig.5. TGA curve of the self-doped polymer h-P(MMA-VTMS).

Fig.6. XRD pattern of self-doped polymer.

Fig.7. The TGA curve of GPEs.

Fig.8. The DSC curve of the self-doped polymer GPE.

Fig.9. XRD patterns (a) $LiClO_4$ and (b) 50wt.% GPE.

Fig.10. AC-impedance spectra of GPEs.

Fig.11. EIS spectra under different temperature (50wt.% GPE).

Fig.12. Temperature dependence of ionic conductivity (50wt.% GPE).

Fig.13. Impedance spectra of the Li/GPE/Li cell measured before and after polarization. (50wt.% GPE)

Fig.14. Electrochemical impedance spectra of the cells Li/50wt.%GPE /Li.

Fig.15. Linear sweep voltammograms (LSV) of the self-doped polymer 50wt.%GPE.

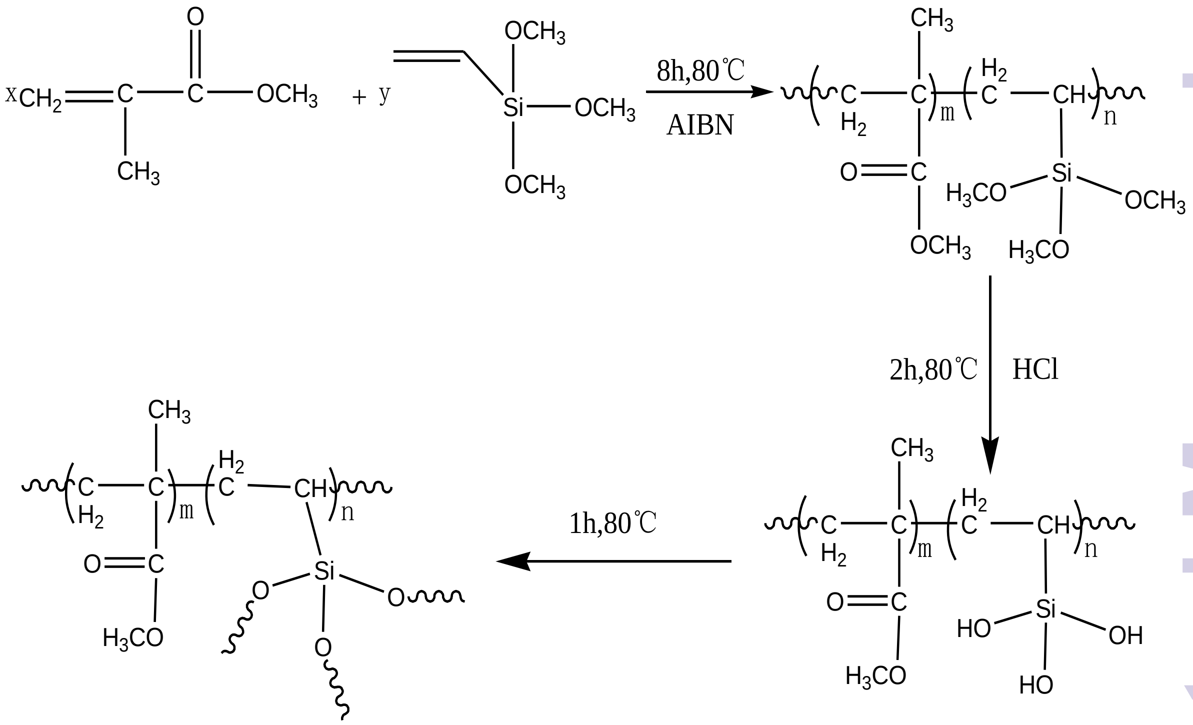

Scheme.1. The ideal synthesis route of the self-doped polymer h-P(MMA-VTMS) (m:n=7:3).

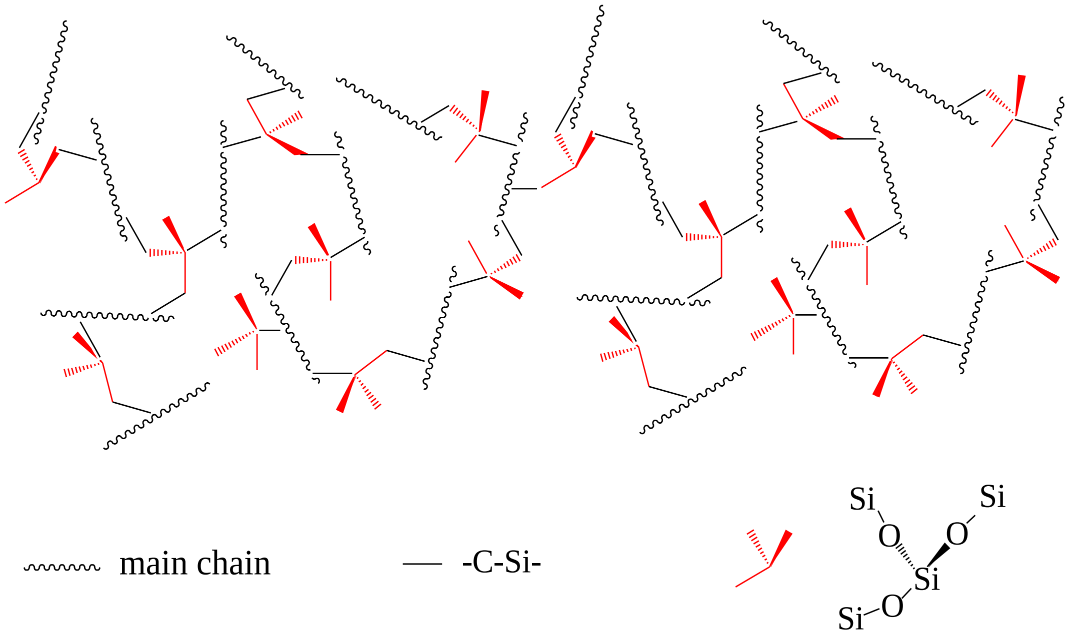

Scheme.2. The ideal structure of the self-doped polymer h-P(MMA-VTMS).

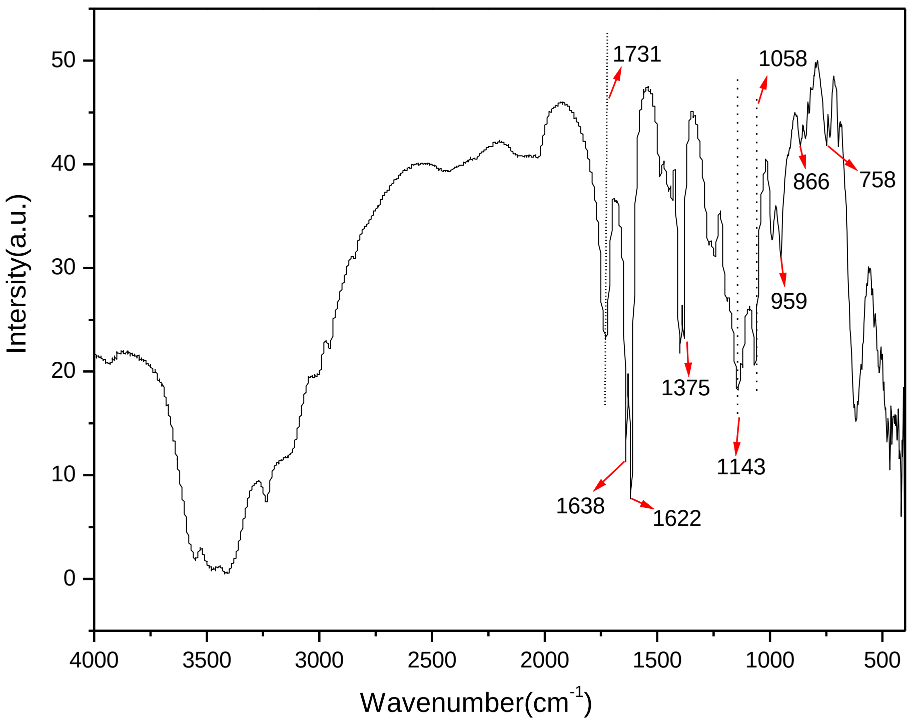

Fig.1. FTIR spectrum of the self-doped polymer h-P(MMA-VTMS).

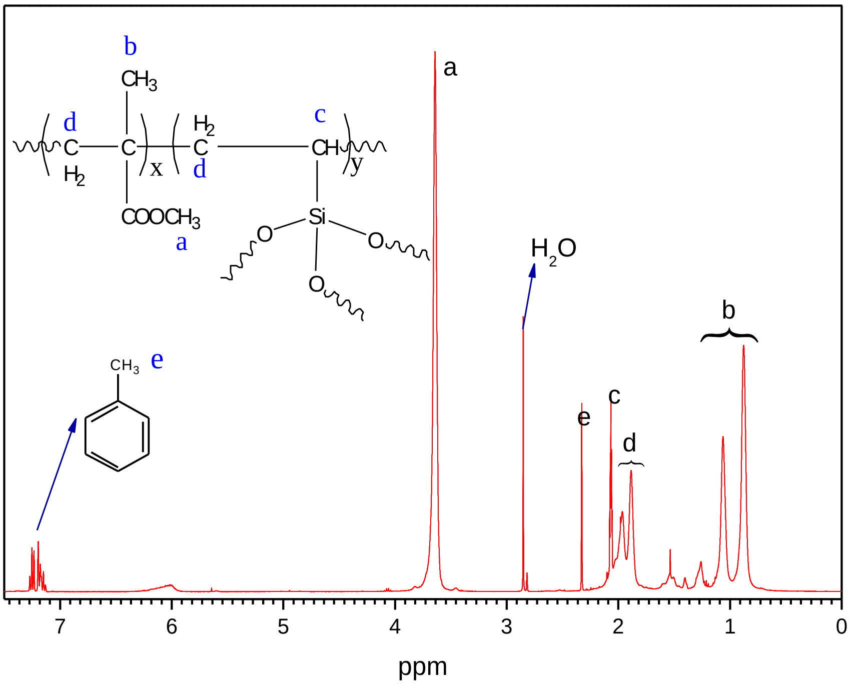

Fig.2. ^{1}H-NMR spectrum of the self-doped polymer of h-P(MMA-VTMS).

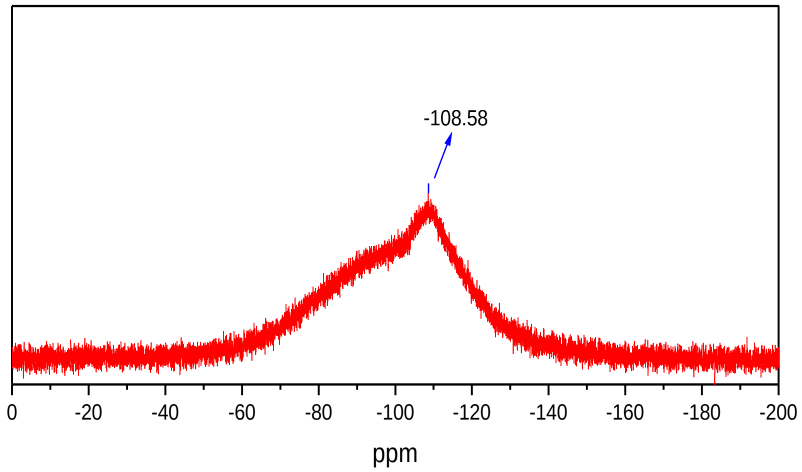

Fig.3. ^{29}Si-NMR spectrum of the self-doped polymer h-P(MMA-VTMS).

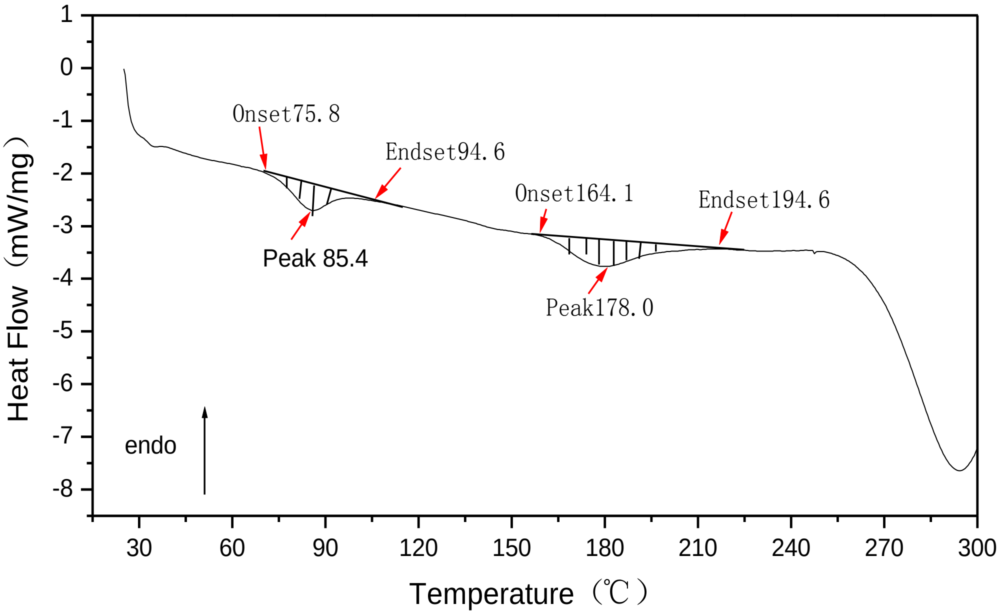

Fig.4. DSC curve of the self-doped polymer of h-P(MMA-VTMS).

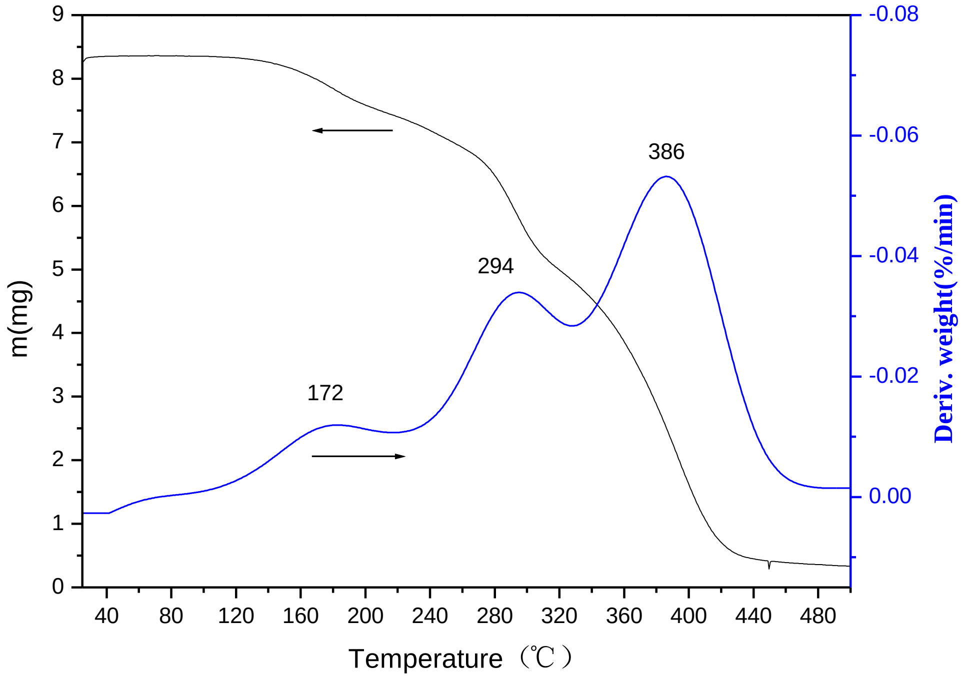

Fig.5. TGA curve of the self-doped polymer h-P(MMA-VTMS).

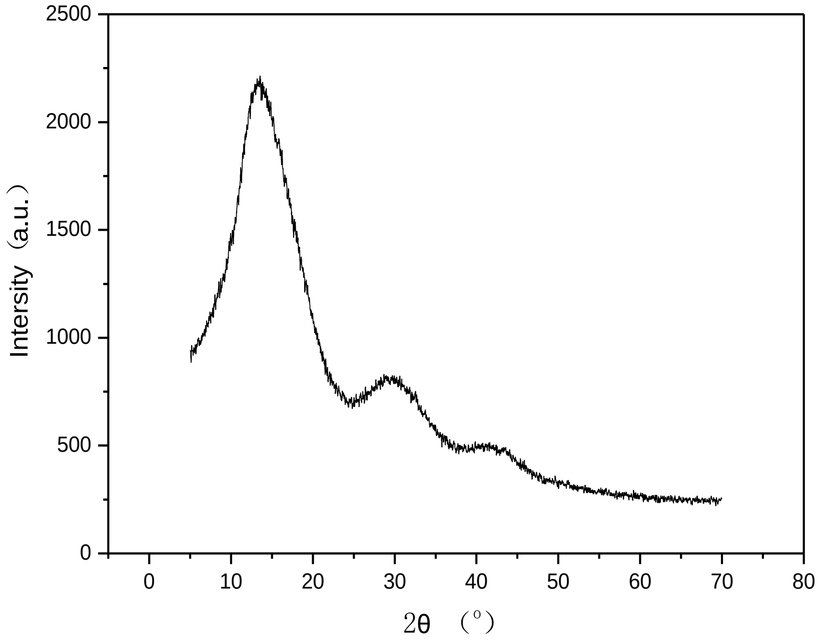

Fig.6. XRD pattern of self-doped polymer

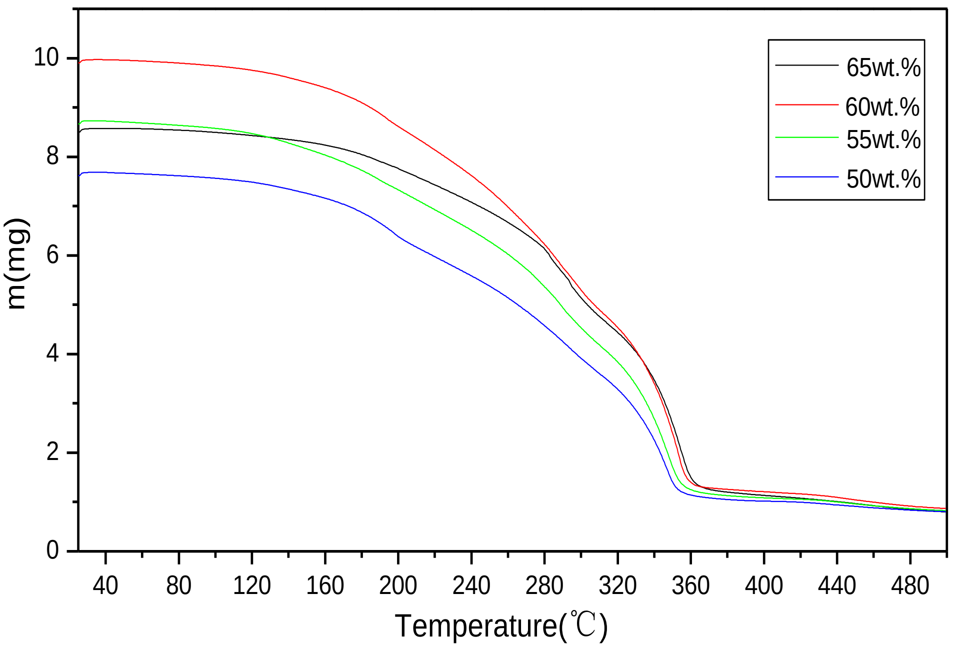

Fig.7. The TGA curve of GPEs.

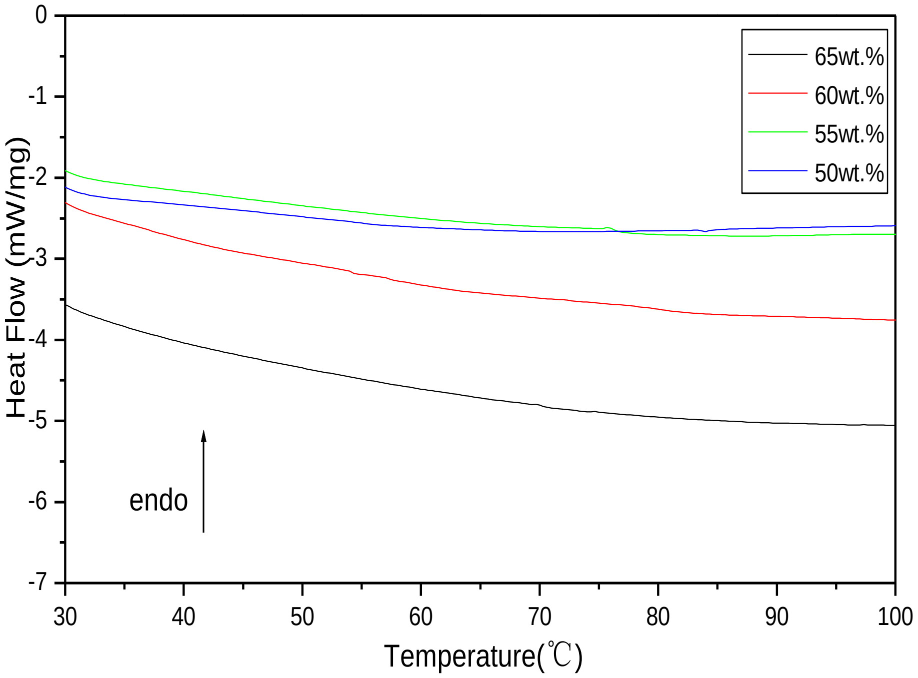

Fig.8. The DSC curve of the self-doped polymer GPE.

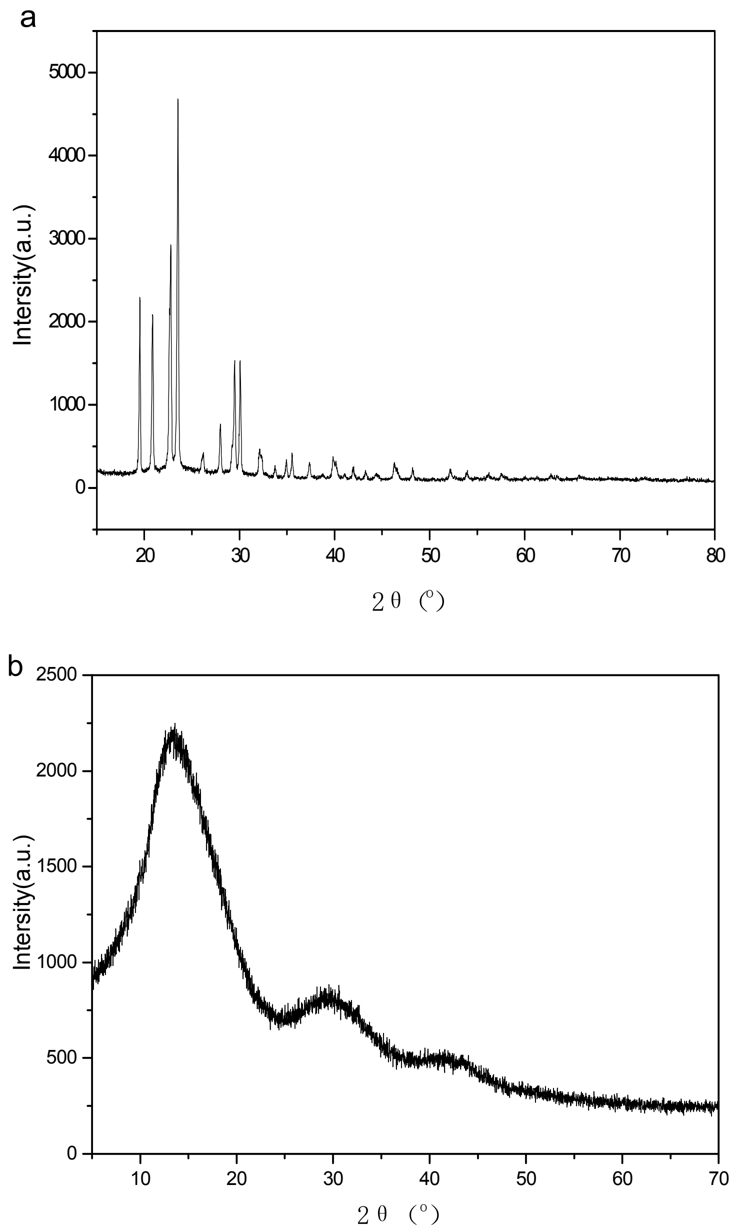

Fig.9. XRD patterns (a) $LiClO_4$ and (b) 50wt.% GPE.

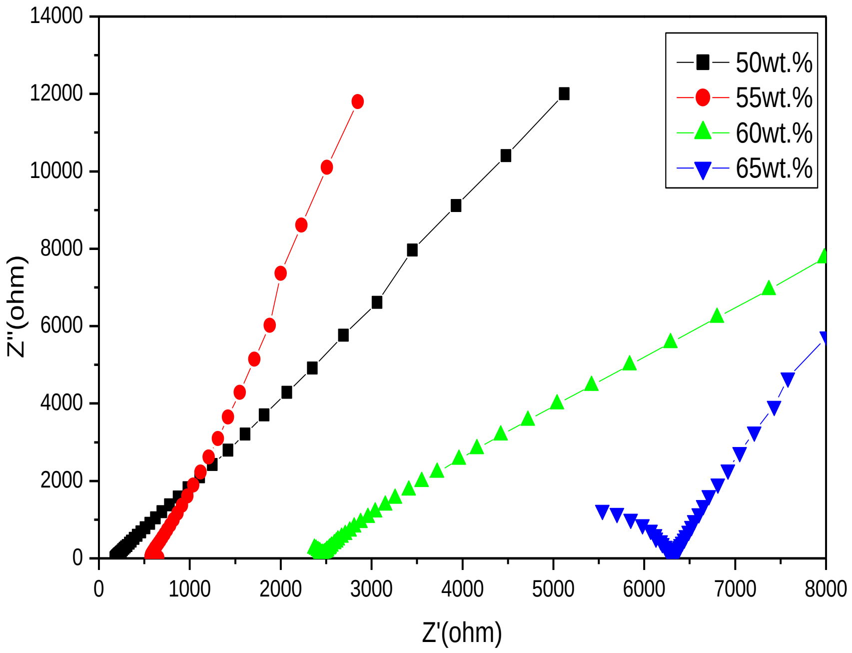

Fig.10. AC-impedance spectra of GPEs.

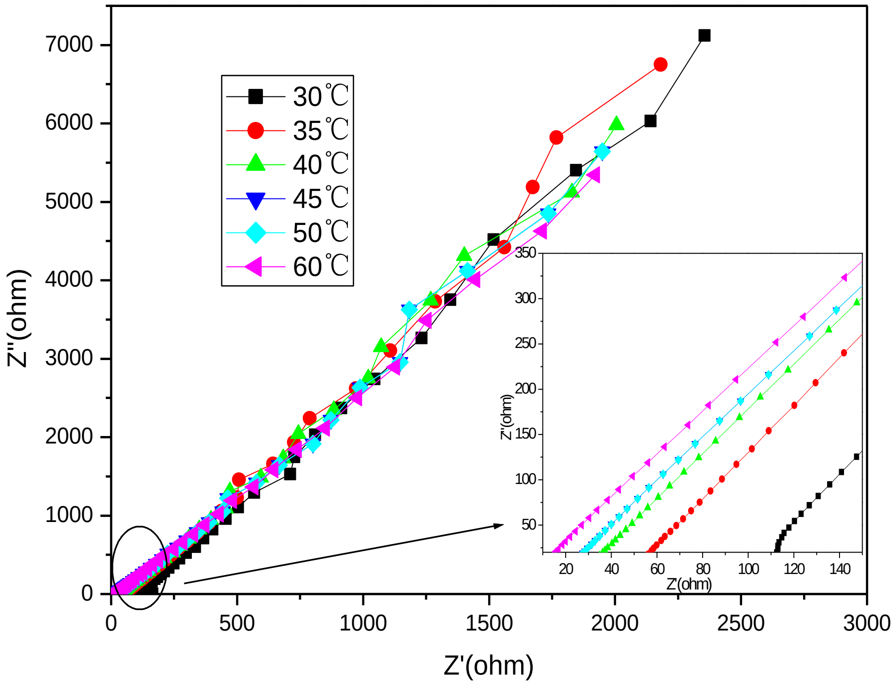

Fig.11. EIS spectra under different temperature (50wt.% GPE).

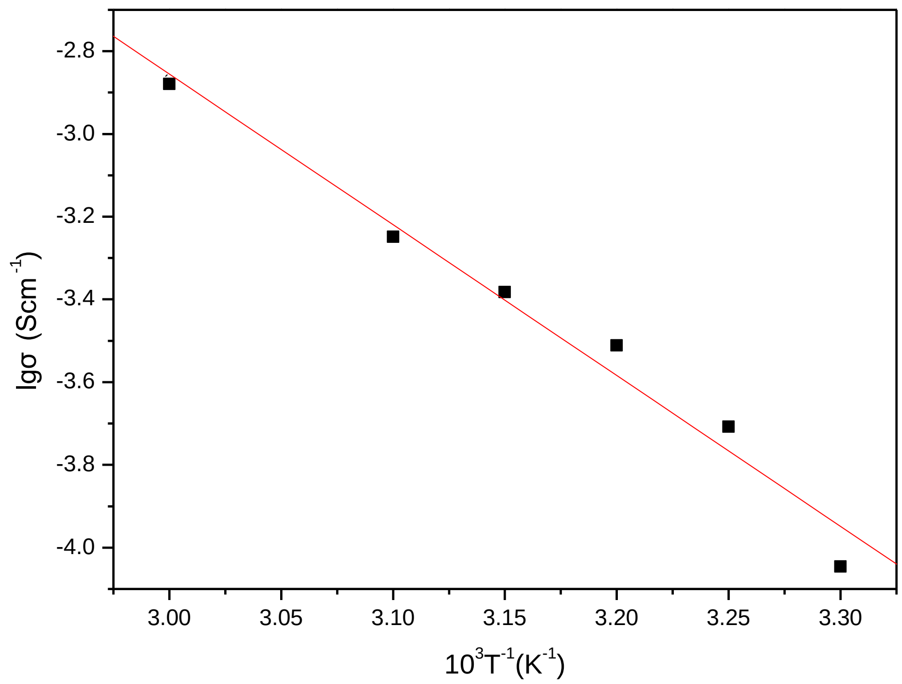

Fig.12. Temperature dependence of ionic conductivity (50wt.% GPE).

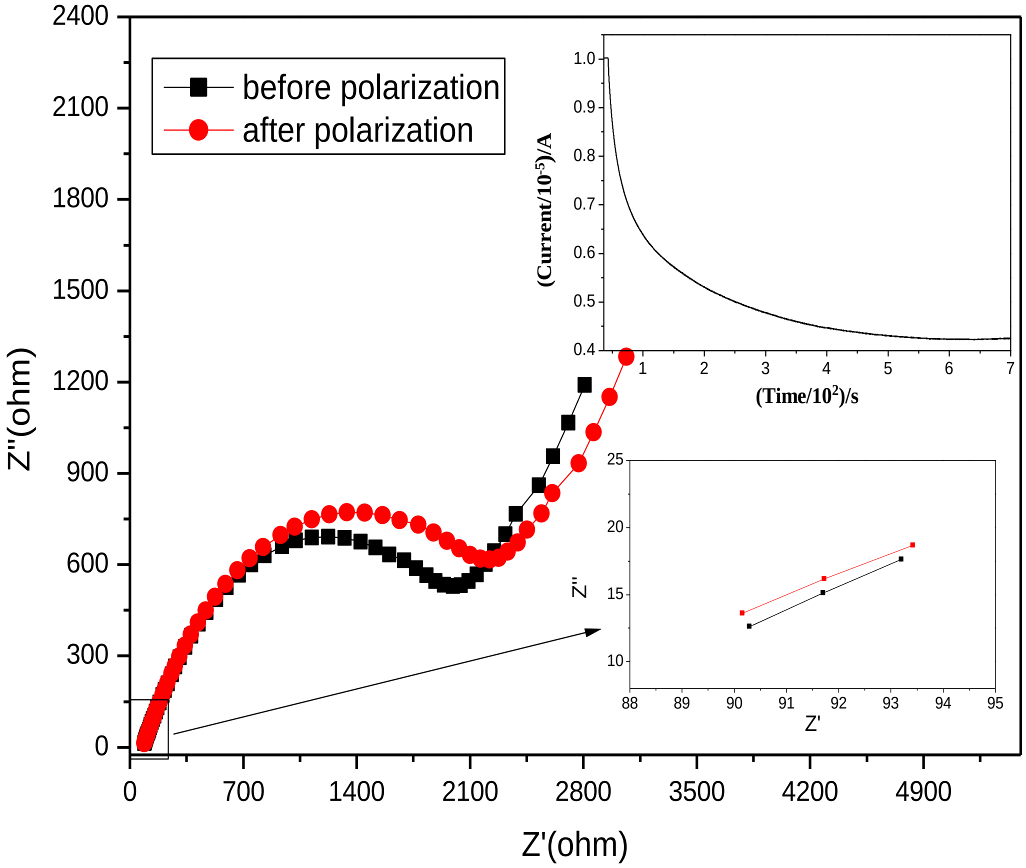

Fig.13. Impedance spectra of the Li/GPE/Li cell measured before and after polarization. (50wt.% GPE)

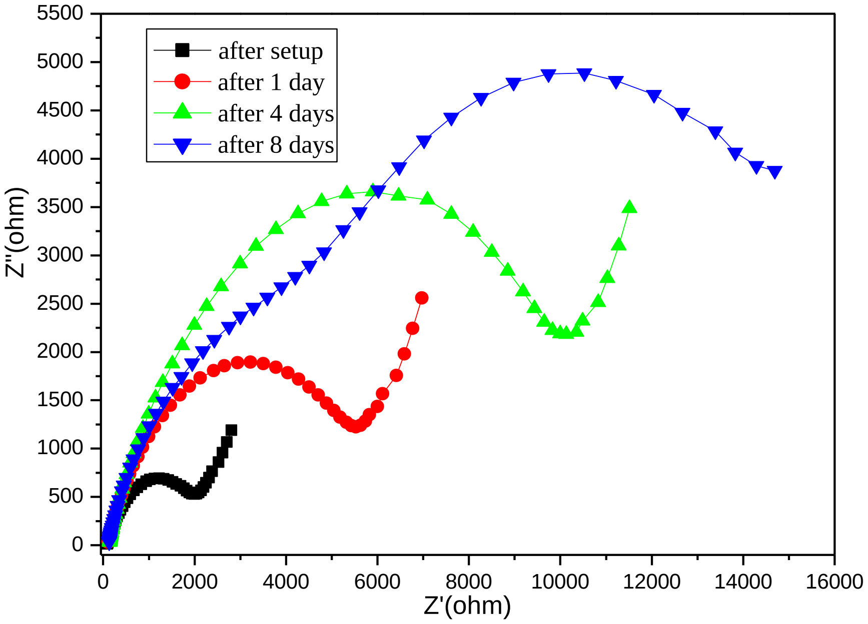

Fig.14. Electrochemical impedance spectra of the cells Li/50wt.%GPE /Li.

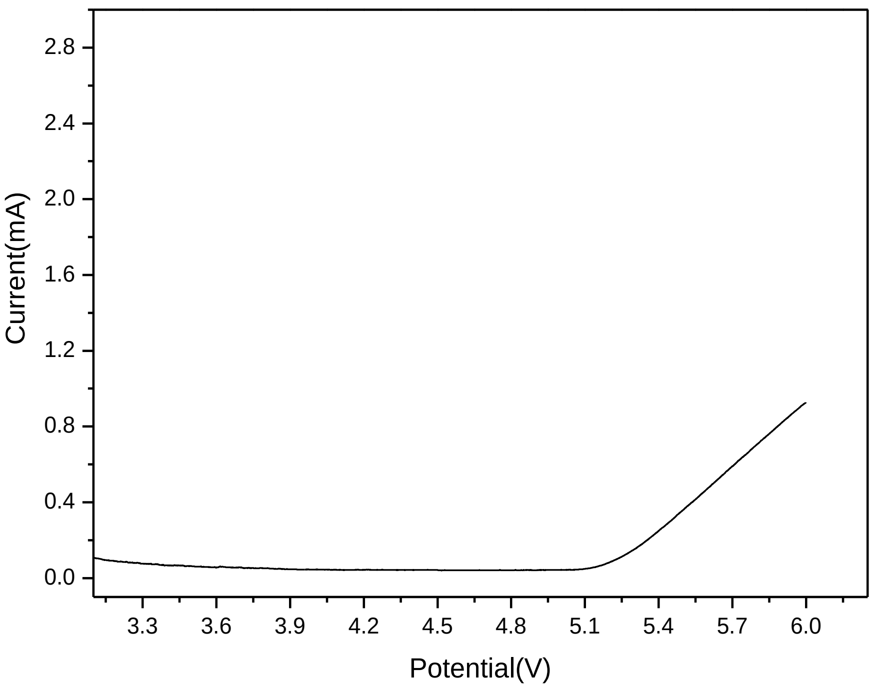

Fig.15. Linear sweep voltammograms (LSV) of the self-doped polymer 50wt.%GPE.